![ELSEVIER]

A pilot study of a simple photon migration model for predicting depth of cure in dental composite

Yin-Chu Chen[a], Jack L. Ferracane[b], Scott A. Prahl[a],*

[a]*Department of Biomedical Engineering, OHSU, 9205 SW Barnes Rd., Portland, OR 97225, USA*
[b]*Division of Biomaterials and Biomechanics, OHSU, Portland, OR, USA*

Abstract *Objectives*. The purpose of this study was to build a photo migration model to calculate the radiant exposure (irradiance $\times$ time) in dental composite and to relate the radiant exposure with extent of cure using polymer kinetics models.
Methods. A composite (Z100, Shade A2) cylinder (21 mm diameter by 15 mm deep) was cured with a tungsten-halogen lamp emitting 600 mW/cm^2, 1 mm above the composite for 60 s. For each of the 2×1 mm grids along the longitudinal cross section (diameter versus depth), the degree of conversion (DC) and hardness (KHN) were measured to construct the curing extent distribution. The inverse adding-doubling method was used to characterize the optical properties of the composite for the Monte Carlo model simulating the photon propagation within the composite cylinder. The calculated radiant exposure (H) distribution along the cross section was related to the curing extent DC/DC_{max} distribution and fitted with two polymer curing kinetics models, the exponential model $DC = DC_{max}[1 - \exp((\ln 0.5)H/H_{dc}^{50\%})]$ and Racz's model $DC = DC_{max}/[1 + (H/H_{dc}^{50\%})^{-2}]$, where $H_{dc}^{50\%}$ is a fitting parameter representing the threshold for 50% of the maximum curing level.
Results and Significance. The absorption and scattering coefficients of uncured composite were higher than that of cured composite at wavelengths between 420 and 520 nm. A roughly hemi-spheric distribution of radiant exposure in the Monte Carlo simulation result was comparable with the curing profiles determined by both DC and KHN. The relationship between *DC* (or *KHN*) and *H* agreed with the Racz model ($r^2 = 0.95$) and the exponential model ($r^2 = 0.93$). The $H_{dc}^{50\%}$ was 1.5(0.1), equal for the two models ($P < 0.05$). The estimated radiant exposure threshold for 80% of the maximum curing level was between 3.8 and 8.8 J/cm^2. The simulation results verify that the radiant exposure extends to a greater depth and width for composite with lower absorption and scattering coefficients.
  Given the optical properties and the geometry of the composite, and the spectrum and the geometry of the light source, the Monte Carlo simulation can accurately

---

* Corresponding author. Tel.: +1 503 216 2197; fax: +1 503 216 2422.
  E-mail address: prahl@bme.ogi.edu (S.A. Prahl).

describe the radiant exposure distribution in a composite material to predict the extent of cure.

Introduction

While significant advances have been made in understanding some of the limitations of dental composites, such as depth of cure, volumetric shrinkage, marginal adhesion, and color stability as well as fracture and wear resistance, there are still many unanswered fundamental questions concerning the light-activated polymerization process. The most important parameter for a light-activated dental composite system is the light-curing efficiency, which is defined as the extent of cure per delivered photon. The light-curing efficiency is affected by several factors, including those related to the composite formulation (monomer type, filler type, composition and size distribution, photosensitizer/accelerator/inhibitor type and concentration), the light source (output spectra, power, time of illumination) and the curing environment (geometry of the specimen, distance from the light source, color of the backing material). These factors affect the absorption and scattering of light, and consequently the amount of light delivered to various depths within the composite.

Many researchers have used an empirical approach to test the light-curing efficiency of composites. Commonly, they measured the extent of cure of the bottom of cured composite disks with different thicknesses (2, 3, 4, and 5 mm) [1] to evaluate different light sources [2-6] or different composition of composites [5-10]. Fourier Transform Infrared (FTIR) spectroscopic analysis has perhaps been the most commonly used method to determine the degree of conversion of light-activated composites [5,11–16]. Another popular parameter, hardness, has also been used routinely to evaluate the depth of cure [3-6,14,17,18]. These methods provide an important indication of the extent of cure, but they do not directly provide information about the exact amount of light absorbed. To date, the exact relationship between the amount of light absorbed by the composite material and the polymerization level has not been fully elucidated.

This study used a Monte Carlo model to simulate photon migration within composite materials to predict the absorbed radiant exposure distribution. The CIE/ISO definition of radiant exposure is the total radiant energy incident on a surface-per-unit area [19]. It is equal to the integral over time of the irradiance [W/cm^2] and has units of J/cm^2. This quantity is often referred in the dental literature as the energy density, which is more accurately defined as the radiant energy per unit volume [J/cm^3] [19]. The radiant exposure varies from point to point in the composite and may be called the radiant exposure distribution. The product of the radiant exposure (at each wavelength) with the absorption coefficient (at the same wavelength) is the absorbed energy density for that wavelength. The integral of all the wavelengths emitted by the lamp is the total absorbed energy per unit volume in the composite.

This radiant exposure distribution depends on the power, the dimension and the position of the light source, and the optical properties and the geometry of the specimen. Based on the relationship between the radiant exposure distribution and the degree of conversion, or between the radiant exposure distribution and the hardness, one can determine the light-curing efficiency for a light-activated composite system. Ultimately, it should be possible to develop a model that can accurately predict the extent of cure of any dental composite in any type of cavity geometry when provided with these parameters.

Materials and methods

Measurement of degree of conversion (DC) and Knoop Hardness (KHN)

The composite material used for this study was a commercially available light-cured minifill dental composite Z100 (Shade A2) having approximately 70 vol.% of zirconia silica filler with average size less than 1 μm (3M ESPE, St Paul, MN, USA). Composite was placed in a 21 mm diameter by 15 mm deep plastic container. A light curing unit (VIP, Bisco Inc., Schaumburg, IL, USA) with a 10 mm diameter light guide was placed 1 mm above the composite. The spectrum of the VIP light curing unit (wavelength range: 400-510 nm) shown in Fig. 1 was measured with a spectrofluorimeter (SPEX Fluorolog-3, Jobin Yvon Inc., Edison, NJ, USA) by directly shining the light into the sample chamber. The composite was
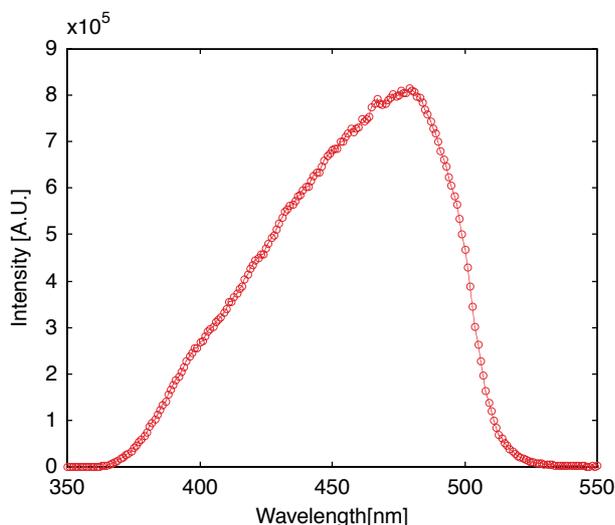
Figure 1 Spectrum of the VIP light curing unit.

illuminated for 60 s at 600 mW/cm^2 measured with a powermeter (Powermax 5200, Molectron, Portland, OR, USA). The powermeter uses a pyroelectric detector and measures the total power emitted from the light, which has a smaller surface area than the detector. The composite was allowed to age for 24 h at ambient temperature in the dark, and was then removed from the plastic container. The uncured, soft material was then scraped away with a knife, and the remaining specimen was embedded in slow-curing epoxy resin (Buehler epoxide, Buehler, Lake Bluff, IL, USA). The embedded composite material was sectioned longitudinally with a slow speed diamond saw (Isomet, Buehler) so that the depth versus the diameter of the cross section was exposed. While it is possible that there would be some absorption of water during this process, the specimens were not tested for hardness immediately afterward, and were stored dry until tested. Therefore, any water would have evaporated from the composite by the time testing commenced. Along the cross section, a grid was drawn on the surface dividing the composite into 2 mm sections across the diameter and 1 mm sections through the depth. Hardness was measured in each 2×1 mm section with a Knoop diamond pyramid (136°). Hardness indentations (Kentron Hardness Tester, Torsion Balance Co., Clifton, NJ, USA) were made on the sectioned surface using a 100 g load and a dwell time of 10 s. Three hardness measurements were made for each grid area and an average hardness value was calculated. The same specimens were then used for the degree of conversion (DC) analysis. Small chips of composite (20–40 µm in thickness and 100 µm in

width and length) removed with a scalpel from the surface of the sectioned sample were placed on a KCl crystal for transmission FTIR (DS20/XAD microscope, Analect Instruments, Irvine, CA, USA). Thirty scans were taken at 8 cm^{-1} resolution. The paste of the uncured composite was similarly tested. DC was calculated from the ratio of the C=C peak from the methacrylate group to that of the unchanging C···C peak from the aromatic ring for the uncured and cured specimens using standard baseline techniques [13]. Three samples were tested for each area on the composite grid, and the results were averaged.

Measurement of optical properties

The inverse adding-doubling (IAD) method [20,21] was used to obtain the absorption μ_a and reduced scattering coefficients μ_s' of both uncured and cured composite. To obtain a disk 1 mm thick and greater than 25 mm in diameter, the uncured composite was placed on a microscope slide and pressed with another microscope slide with 1 mm spacers in between. This was done in the dark and the uncured composite disk samples were covered with aluminum foil. To obtain cured composite samples, the VIP light curing unit set to 600 mW/cm^2 was used to cure the disk samples. To ensure complete curing of the whole sample, both sides of the disk were illuminated for more than two minutes.

The reflection spectra of the samples were measured with an 20.3 cm diameter integrating sphere (IS-080, Labsphere Inc., North Sutton, NH, USA) in a reflectance mode configuration (Fig. 2a). A high-intensity lamp (Fiber-Lite High Intensity Illumination Series 180, Dolan-Jenner Industries, Inc., Lawrence, MA, USA) was used for illumination. Light from the lamp was conducted through a 600-µm diameter optical fiber (FT600ET, Thorlabs, Newton, NJ, USA) inserted in a stainless steel tube (painted white on the surface) and positioned 5 mm from the sample. The reflection signal was collected by a 1000-µm diameter optical fiber placed at the 0.64-cm. diameter port of the sphere, guided to a spectrofluorometer (SPEX Fluorolog-3), and was recorded from 400 to 700 nm (1 nm bandpass, 0.1 s/nm). The sample was placed at the 2.54-cm diameter port of the sphere. Reference standards with 50, 75, and 99% reflectance (Spectralon, Labsphere Inc., North Sutton, NH, USA), and rough-surface black paper (as 0% reflectance) were measured for the calibration of the lamp. All the measurements were done in the dark. A total of five samples were measured.

Transmission measurements were similar to the reflection measurements except that the light
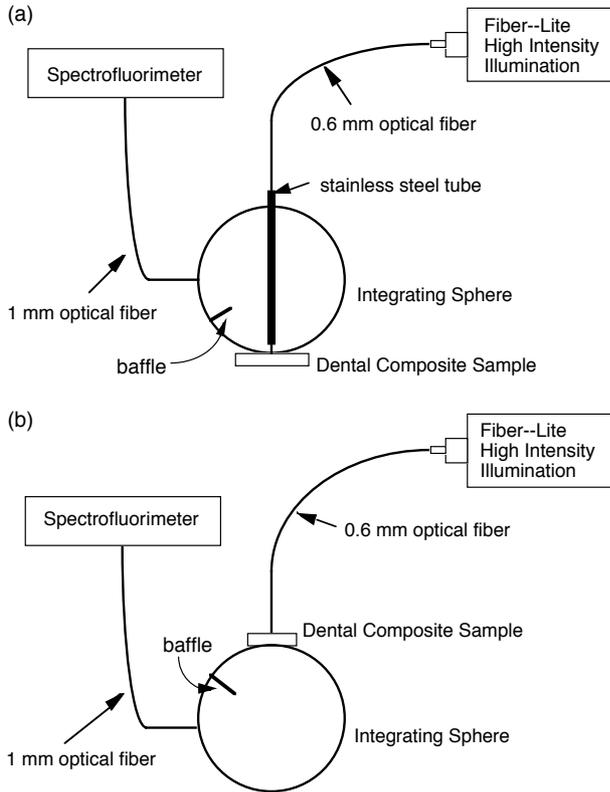
Figure 2 Experimental setup for optical property measurements. (a) Is the configuration for measuring reflectance and (b) is used to measure transmission.

illumination was from outside the integrating sphere (Fig. 2b). For calibration, 0 and 100% transmission were measured by putting aluminum foil or nothing at the transmission port of the sphere.

The reflectance of samples was calculated using

$$R_{sample} = R_{std} \frac{M_{R(sample)} - M_{R(dark)}}{M_{R(std)} - M_{R(dark)}}$$

where R_{sample} is the reflectance of the sample, $M_{R(sample)}$ is the reflection spectrum of the composite sample, $M_{R(dark)}$ is the reflection spectrum of the rough-surface black paper, $M_{R(std)}$ is the reflection spectrum of the reflectance standard, and R_{std} is 0.99 for 99% reflectance standard, 0.75 for 75% reflectance standard, and 0.5 for 50% reflectance standard. The transmission was calculated using

$$T_{sample} = \frac{M_{T(sample)} - M_{T(Al)}}{M_{T(100)} - M_{T(Al)}}$$

where T_{sample} is the transmittance of the sample, $M_{T(sample)}$ is the transmission spectrum of the composite sample, $M_{T(Al)}$ is the transmission spectrum of the aluminum foil, and $M_{T(100)}$ is the transmission spectrum of nothing.

The reflectance R_{sample} and transmittance T_{sample} values were then fed into the IAD software program to extract the intrinsic optical parameters for the samples. The program does this by repeatedly estimating the optical properties and comparing the expected observations with those obtained experimentally [20].

Monte Carlo simulations

A Monte Carlo computer model was developed to simulate the photon migration in the composites. The Monte Carlo method is often used to simulate light transport in tissue [22–25]. Monte Carlo refers to a technique first proposed by Metropolis and Ulam to simulate physical processes using a stochastic model [26]. In a radiative transport problem, the Monte Carlo method consists of recording photon histories as they are scattered and absorbed. Very sophisticated Monte Carlo programs have been developed; many have been used to simulate laser tissue interactions. Fig. 3 shows a flowchart of the steps involved in propagating a photon packet. Once the photon packet is launched, it is moved to the next scattering or absorption event. The photon packet may propagate undisturbed or interact with the boundaries. Photons are absorbed by the composite based on
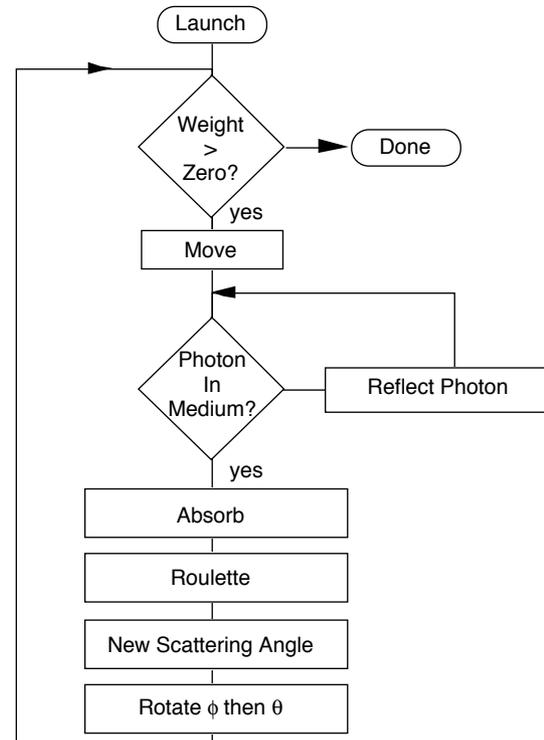
Figure 3 Monte Carlo steps to simulate photon packets in dental composite. The roulette step is used to terminate the photon packet in an unbiased manner.

the absorption properties of the material. When photons hit the top surface of the specimen, they are either transmitted to the air or reflected back into the sample. The chance of reflection depends on the Fresnel reflection at the particular angle of incidence [27].

The number of photons in the packet is called the *weight* and is modified at each interaction. The photon packet is repeatedly moved until it is completely absorbed or escapes from the composite. A new photon packet is launched and this process is repeated until the desired number of photons has been propagated. The recorded reflection, transmission, and absorption profiles approach the true values as the number of photons propagated approaches infinity. The amount of light per area is obtained by dividing the absorbed energy (J/cm^3) by the absorption coefficient (cm^{-1}) to obtain the light dose at each point in the sample (J/cm^2).

A 10 mm diameter collimated, round flat beam was launched normal to the sample. The sample was set to 20 mm wide, 20 mm long and 10 mm deep, and divided into $(1 \times 1 \times 1)$ mm^3 cubic bins to record the absorbed photon energy. The optical properties were held constant during each simulation. Photons that hit an outer boundary other than the top surface were terminated and their energy was deposited into the last bin they occupied. A total of 10^7 photons were launched for each simulation.

In the DC and KHN experiment, the total energy of light delivered was (the irradiance)×(duration of illumination)×(the total area of light source)= 600 mW/cm^2×60 s×$\pi(0.95/2)^2$ cm^2=25.5 J. The final absorbed photon count of each bin in the Monte Carlo simulation was divided by the total number of launched photons, the bin volume, and the absorption coefficient, and then multiplied by 25.5, so the final values represented the radiant exposure distribution (J/cm^2) in the composite. This distribution was then compared with the DC and KHN distributions.

Since the optical properties of the uncured and the cured composite were different, two sets of simulations were performed. These two simulations should bracket the range of possible light distributions for samples whose optical properties dynamically change during curing. Since the lamp emission peak (Fig. 1) and the camphorquinone absorption peak [28] fall in the wavelength region of 470(5) nm, the optical properties were set as follows: $\mu'_s = 13.67$ cm^{-1}, $\mu_a = 1.06$ cm^{-1} for uncured samples, and $\mu'_s = 12.76$ cm^{-1}, $\mu_a = 0.68$ cm^{-1} for cured samples (see Fig. 4 in Results section). The refractive index was set at $n = 1.49$ for both uncured and cured samples. The exact refractive
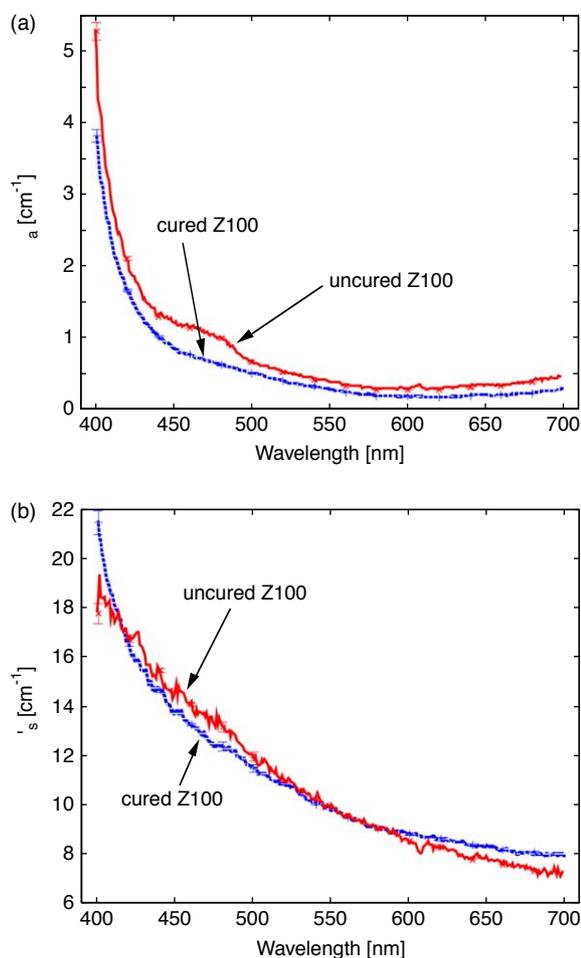
Figure 4 (a) Is the absorption coefficient μ_a as a function of wavelength of uncured (solid) and cured (dashed) dental composite Z100. (b) Is the reduced scattering coefficient μ'_s as a function of wavelength of uncured (solid) and cured (dashed) Z100.

indices, which may be different between the uncured and the cured composite, were not measured. In the Monte Carlo simulations, 1% of the refractive index variation affects about 1% of the chances of reflection at the top surface. Increasing the refractive index increases the chance of the reflection, which, in turn, increases the chance of the photons propagating in the composite.

Relating Monte Carlo radiant exposure with DC and KHN

The radiant exposure at each position in the sample was compared with the measured DC and KHN values. Various nonlinear models have been proposed to describe polymer curing kinetics [29-31]. In this paper, three simple models were adapted to fit the relationship between the extent of cure and the radiant exposure.

Exponential Model

The first one is a commonly used [7,18,32], one-phase, two-parameter, exponential form model,

$$\frac{M(0) - M(t)}{M(0)} = 1 - \exp(-kt),$$

where $M(0)$ is the initial concentration of methacrylate groups, $M(t)$ the concentration of methacrylate groups at time t (the exposure time), and k is a rate parameter. Since the radiant exposure (J/cm^2) is equal to the product of the irradiance (W/cm^2) and the time (s), we replaced the time of light exposure t with the radiant exposure H, and replaced the fitting parameter, k, with $H_{dc}^{50\%}$ and $H_{khn}^{50\%}$ to include the concept of the curing threshold for 50% of maximum degree of conversion and Knoop hardness. Therefore, the above equation was rewritten as (called 'exponential model' in this paper)

$$DC = DC_{max}\left(1 - \exp\left(\ln 0.5\frac{H}{H_{dc}^{50\%}}\right)\right), \tag{1}$$

$$KHN = KHN_{max}\left(1 - \exp\left(\ln 0.5\frac{H}{H_{khn}^{50\%}}\right)\right).$$

Racz Model

The second model was proposed by Racz [30]. It can be expressed as

$$\frac{M(0) - M(t)}{M(0)} = \frac{kt^n}{1 + kt^n},$$

where t is the curing time, and k and n are the fitting parameters. This model allows a S-shaped curve. Similarly, t can be correlated with radiant exposure H, and k with radiant exposure threshold, $H_{dc}^{50\%}$ and $H_{khn}^{50\%}$, as 50% of the maximum curing level. Moreover, in our result, the best fit for n was about 2(0.2) for both DC and KHN data. Therefore $n=2$ was fixed for both the uncured and cured composite. The formulation can then be rewritten as

$$DC = DC_{max}\frac{(H/H_{dc}^{50\%})^2}{1 + (H/H_{dc}^{50\%})^2}, \tag{2}$$

$$KHN = KHN_{max}\frac{(H/H_{khn}^{50\%})^2}{1 + (H/H_{khn}^{50\%})^2}.$$

Watts Model

Watts has described an expression for the polymerization kinetic model of light activated resin composite [29],

$$\frac{DC}{DC_{max}} = 1 - \exp[-k_p k_t^{-0.5}(\Phi I_a)^{0.5}t],$$

where k_p and k_t are the propagation and termination rate constants, Φ is the quantum yield for initiation, I_a is the light fluence rate absorbed by the photosensitizer, and t is the exposure time. If all the material dependent parameters ($k_p k_t^{-0.5}\Phi^{0.5}$) are combined into a single constant α, then the above equation can be rewritten as

$$\frac{DC}{DC_{max}} = 1 - \exp(-\alpha I_a^{0.5}t).$$

If $H = I_a t$ and we let $H_{dc}^{50\%} = -\alpha^{-2}t^{-1}(\ln 0.5)^2$, then for a constant exposure time t we obtain

$$\frac{DC}{DC_{max}} = 1 - \exp[\ln 0.5(H/H_{dc}^{50\%})^{0.5}], \tag{3}$$

where once again $H_{dc}^{50\%}$ represents the radiant exposure to reach 50% of the maximum cure.

Results

Optical properties of dental composite

Fig. 4a shows that the absorption coefficient μ_a of the composite decreases as the wavelength increases, and decreases upon curing, especially at wavelengths between 440 nm and 500 nm. For the wavelength region of 470(2) nm, which corresponds to the lamp emission peak and the camphorquinone absorption peak [28], the absorption coefficient is 1.06(0.02) cm^{-1} for uncured Z100, and 0.68(0.02) cm^{-1} for cured Z100.

Fig. 4b shows the reduced scattering coefficient μ_s' of cured and uncured composites as a function of wavelength. Observe that the uncured composite has a slightly higher scattering coefficient than the cured composite in the wavelength range of 420-550 nm. The scattering coefficient for both cured and uncured composites decreases as the wavelength increases. For the wavelength region 470(2) nm, the reduced scattering coefficient is 13.67(0.05) cm^{-1} for uncured Z100, and 12.76(0.04) cm^{-1} for cured Z100.

DC, KHN and Monte Carlo simulation

Fig. 5 depicts the Knoop Hardness number (KHN) versus the DC in a linear relationship with a coefficient of determination $r^2 = 0.757$. Fig. 6 compares the measured DC and KHN values and the Monte Carlo radiant exposure across the uncured and cured sample. The averaged coefficients of variation (SD/mean) of the experimental errors are 7% for the KHN values and 5% for the DC values. Note that the DC contour map shows that the
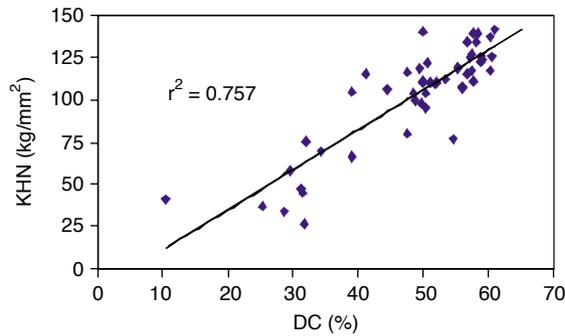
Figure 5   The Knoop hardness number versus the degree of conversion. The coefficient of determination r^2 between the data and the regression line is 0.757.
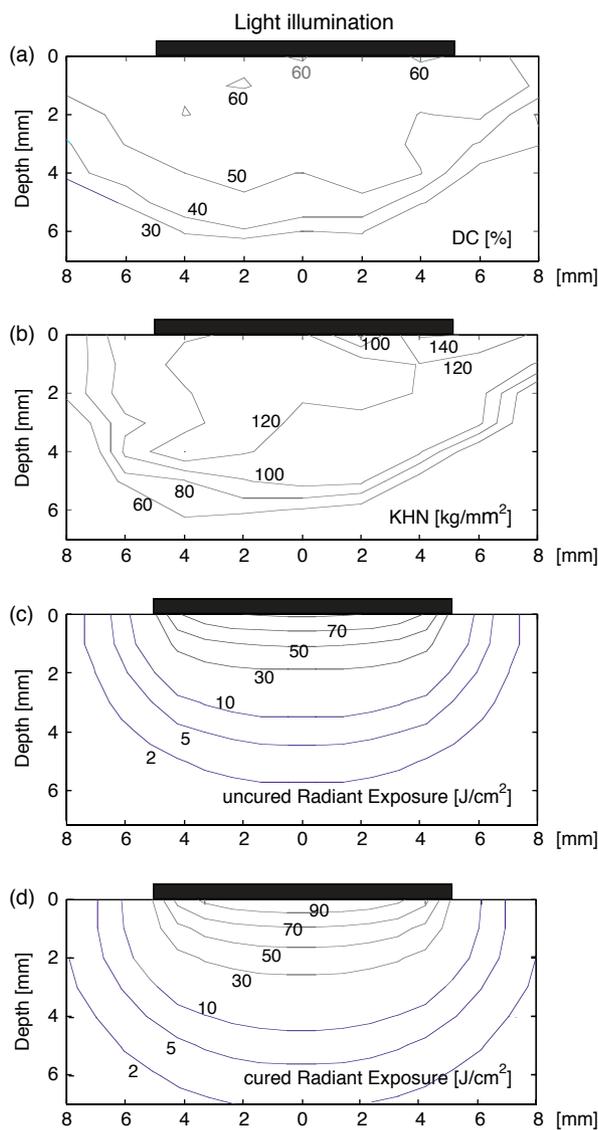
Figure 6   Distributions of measured DC (a), KHN (b), and calculated Monte Carlo radiant exposure for uncured (c) and cured (d) composite. The black bar above each contour map indicates the extent of the curing beam.
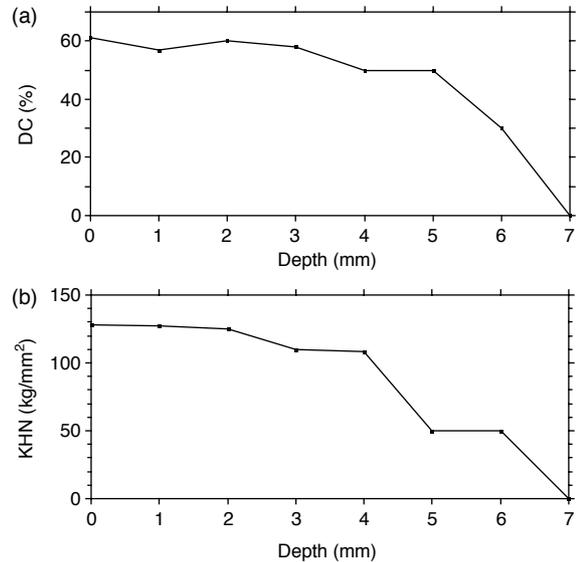
Figure 7   (a) The DC versus depth along the central position ($x = 0$ mm in Fig. 6(a)). (b) The KHN versus depth along the central position ($x = 0$ mm in Fig. 6(b)).

composite reached the 80% curing level (DC $\approx$ 50%) down to a depth of 4 mm and roughly 8 mm in radius, while the KHN contour map shows that the 80% curing level (KHN $\approx$ 110 kg/mm^2) extended to slightly greater than 4 mm in depth and 6 mm in radius. The depth for 50% of the maximum DC (DC $\approx$ 30%) and KHN (KHN $\approx$ 70 kg/mm^2) extends down to about 6 mm. The DC and KHN as a function of depth were plotted in Fig. 7.

Relating Monte Carlo radiant exposure to DC and KHN

The measured DC and KHN values at each point in the sample were plotted against the calculated radiant exposure at that point and were fitted with exponential and Racz models for an uncured composite (Fig. 8) and for a cured composite (Fig. 9). Additionally, the distribution of the DC versus radiant exposure for the uncured composite was fitted with Watts' model (Fig. 8a). The best fits based on those models for $H_{dc}^{50\%}$ and $H_{khn}^{50\%}$, and the calculated radiant exposure $H_{dc}^{80\%}$ and $H_{khn}^{80\%}$ for the 80% curing level, are listed in Table 1. There was no significant difference between exponential and Racz models for all the thresholds, $H_{dc}^{50\%}$, $H_{khn}^{50\%}$, $H_{dc}^{80\%}$, and $H_{khn}^{80\%}$, based on one-way ANOVA followed by Tukey's post-hoc multiple comparison test at $P < 0.05$. However, the $H_{dc}^{50\%}$ in Watts' model was shown to be 1.68 with 0.26 standard error (Fig. 8a), which is about 15% standard error, therefore this fit was not as good as the other two models (7% standard error).
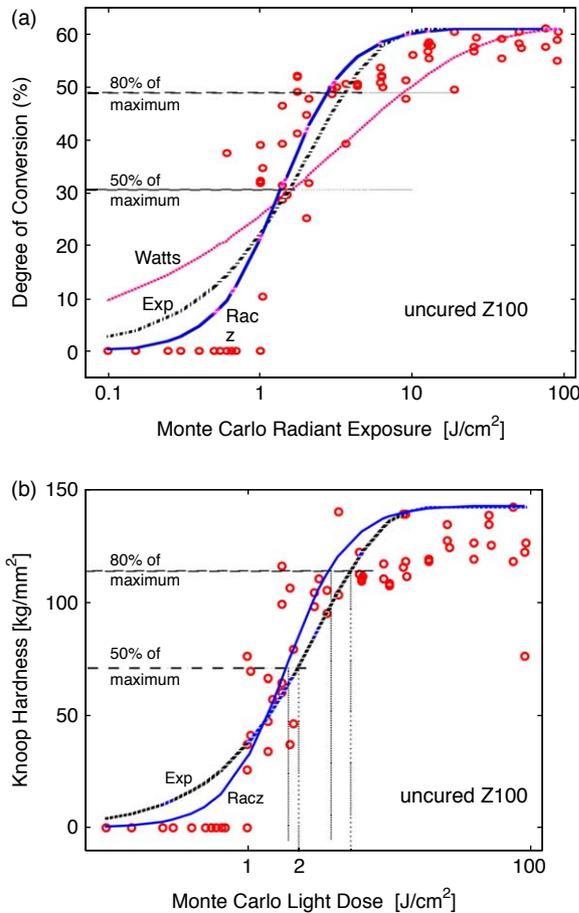
Figure 8 The circles are the data of DC (a) and Knoop Hardness (b) versus Monte Carlo radiant exposure for uncured Z100. The curves are fitted with the Racz model (solid), the exponential model (dashed), and Watts model (dashdot). The coefficient of determination r^2 for the fitted curve was 0.93 for the exponential model and 0.95 for the Racz model.

Discussion

Few groups have studied the optical properties of dental composite. Lee et al. measured the photometric properties based on two geometries of total reflectance measurements [33]. This photometric technique was useful for evaluating the esthetic appearance of the materials, but lost detail with respect to how the composite interacts with each wavelength because it measured an integrated parameter (e.g. lumping all green wavelengths together). Taira et al. measured Kubelka-Munk optical coefficients [34]. However, it is difficult to relate these coefficients to the standard optical properties [35,36]. In this study, the standard absorption and scattering properties of the composite before and after curing were measured [37], because these intrinsic optical properties can be used in light propagation models.
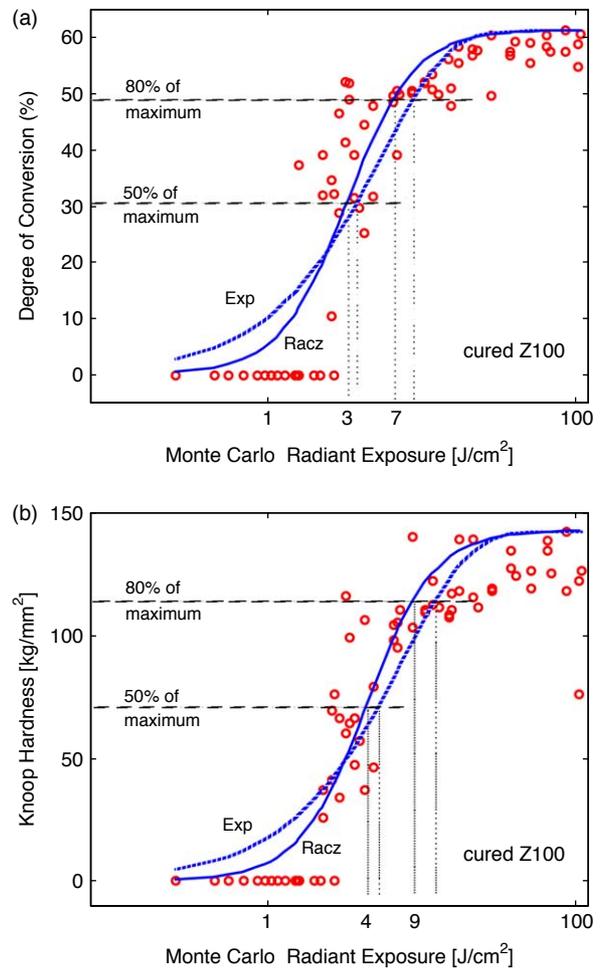
Figure 9 DC (a) and Knoop Hardness (b) versus Monte Carlo radiant exposure for cured Z100. The solid curve is fitted with the Racz model, and the dashed curve is fitted with the exponential model. The coefficient of determination r^2 for the fitted curve was 0.92 for the exponential model and 0.94 for the Racz model.

Fig. 6 shows that the DC level contour is slightly wider laterally than the KHN level contour. For the region depth smaller than 4 mm, KHN had more layers than DC. Moreover, the 50% DC contour reaches a slightly lower depth than the 50% KHN contour. In fact, the distribution between the DC and the KHN only moderately fits a straight line with the coefficient of determination $r^2 = 0.757$ (Fig. 5). The figure also indicates that while curing the Z100, the increasing of KHN lags behind increasing DC at the initial stage of polymerization and after 80% of the total conversion has been achieved, a greater increase in KHN occurs while changes in DC are subtle. A similar result was found by Ferracane [14], who measured the DC and KHN of three unfilled resins. It was found that despite there being a good correlation between increasing hardness and increasing DC during the setting reaction, the

Table 1   The optical properties used in the Monte Carlo simulation for uncured and cured Z100, and the comparison of the fitting parameters, $H_{dc}^{50\%}$ and $H_{khn}^{50\%}$, and the calculated radiant exposure thresholds, $H_{dc}^{80\%}$, and $H_{khn}^{80\%}$ using the exponential and the Racz model.

	Uncured			Cured	
	Exponential	Racz	Watts	Exponential	Racz
μ_a (cm^{-1})		1.06(0.02)		0.68(0.02)	
μ_s' (cm^{-1})		13.67(0.05)		12.76(0.04)	
$H_{dc}^{50\%}$ (J/cm^2)	1.5(0.1)	1.4(0.1)	1.68(0.26)	3.8(0.3)	3.3(0.2)
$H_{khn}^{50\%}$ (J/cm^2)	2.3(0.2)	1.9(0.1)		5.2(0.4)	4.4(0.3)
$H_{dc}^{80\%}$ (J/cm^2)	3.6(0.3)	2.8(0.2)	9.0(1.4)	8.7(0.7)	6.7(0.4)
$H_{khn}^{80\%}$ (J/cm^2)	5.3(0.4)	3.8(0.2)		12.0(1.0)	8.8(0.6)

The $H_{dc}^{50\%}$ and $H_{dc}^{80\%}$ values from Watts model were listed as a comparison. Values are mean radiant exposure. The standard errors of the means are in parentheses.

acquisition of hardness chronologically lags behind the conversion of carbon double bonds. This perhaps can be explained by the fact that at the initial stage of polymerization, a much greater percentage of carbon double bonds are reacted to form polymer chains than are reacted to crosslink existing chains, thereby the relatively smaller polymer chains do not provide sufficient hardness increases. However, as the composite reaches the maximum curing (DC > 50%), a complex polymer network has been formed. Therefore, only a small change of DC, corresponding to further extensive crosslinking between polymer chains, causes a large increase in hardness [14]. The DC and KHN drop rapidly at a depth greater than 5 mm (Fig. 7). A similar decrease of composite Barcol hardness was found by Mills et al. [38]. It appears that the decrease followed an exponential function.

Overall, the roughly hemi-elliptical shape of the curing level (Fig. 6a,b) was comparable to that of the light dose distribution (Fig. 6c,d). It is interesting to see that for those curing levels greater than 80% (depths less than 4 mm), the Monte Carlo light dose distribution shows more layers of light dose than the KHN distribution, which, in turn, has more layers of KHN values than DC. This can be explained by the fact that when the composite is converted (adequately cured), its DC and KHN values reach ≥ 80% of the maximum value and begin to saturate, while in the Monte Carlo simulations, the photon can be accumulated continuously.

The DC and KHN level contours were slightly asymmetrical with respect to the center, that is the left side shows deeper depth of cure than the right side, (Fig. 6a,b). This was due to the slight asymmetrical light distribution from the center of the LED-curing lamp. The model result, which shows symmetrical distribution along the center, did not take asymmetrical light distribution into

account. This may cause discrepancy between the experiment and the model.

Fig. 6 shows that the 80% cure region was wider than the region directly illuminated by the curing light guide. This is primarily a result of scattering by the composite. While it is possible that beam divergence may occur, this measurement showed that the beam diverged only 1 mm over a distance of 7 mm in air. Divergence would be even less in the higher index of refraction composite. To examine how the scattering and absorption coefficients affect the light distribution, another two simulations were performed with optical properties set to the same values as uncured Z100, but with doubled scattering or doubled absorption. Comparing both results (Fig. 10b,c) with the original uncured Z100 radiant exposure (Fig. 10a), one can see that a higher scattering coefficient translates to higher radiant exposures in the central direct-illumination region, while a higher absorption coefficient yields lower radiant exposures at the center. Light in both samples penetrates less deeply and less laterally, and would have less width and depth of cure. Visible light should penetrate better than UV light because Z100 has a lower scattering and absorption coefficient at longer wavelengths (Fig. 4).

The fit between the extent of cure (DC or KHN) and the Monte Carlo radiant exposure in Fig. 8 and 9 yielded a slightly greater coefficient of determination r^2 value (0.95 on average) using the Racz model than for the exponential model ($r^2 = 0.93$ on average). Cohen et al. [18] also used the exponential model and Racz's model to fit the KHN versus the exposure duration distribution, and they also found a slightly higher coefficient of determination for the Racz model than the exponential model. The fit using the Watts model only yielded a coefficient of determination $r^2 = 0.79$. However, it is interesting to note that the 50%-curing thresholds ($H_{dc}^{50\%}$) are
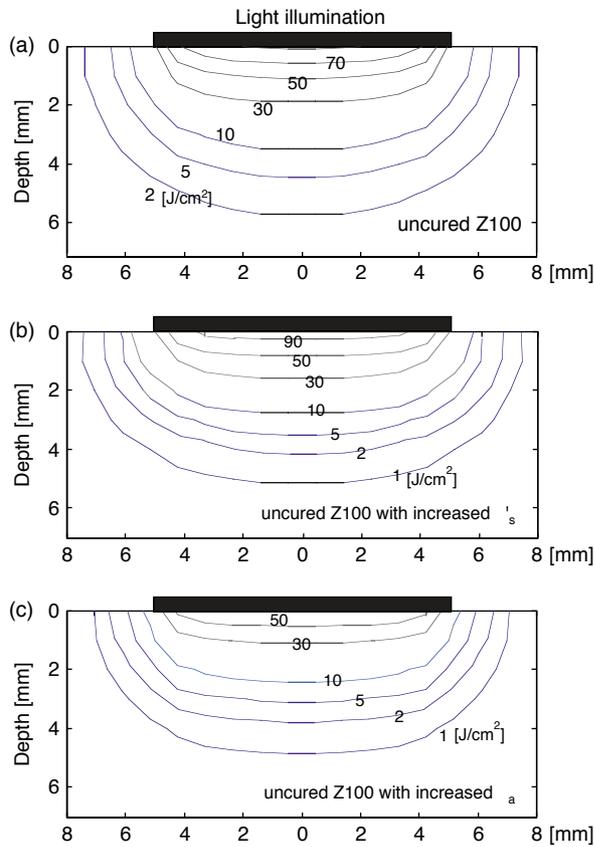
Figure 10 Monte Carlo radiant exposure of composites with optical properties of uncured Z100 (a), doubled scattering (b), and doubled absorption (c).

equal in all three models based on one-way ANOVA followed by Tukey's post-hoc multiple comparison test at $P < 0.05$. The three fitting curves cross at $DC \approx 28\%$ (Fig. 8), but the slopes of the three curves at $DC \approx 28\%$ differ and have the following order: Racz > exponential >> Watts. As a result, the estimated radiant exposure threshold for the 80%-curing level ($H_{dc}^{80\%}$) in the Watts model differs significantly from the $H_{dc}^{80\%}$ in the other two models (t-test: $P < 0.05$).

Including $H^{50\%}$ in the mathematical expressions for the models gives the advantages of unifying all the physical parameters (e.g. two in the Racz model, and four in the Watts model) into a single fitted parameter with a practical unit (J/cm^2). Moreover, the 80% curing threshold can be obtained by simply multiplying $H^{50\%}$ by 2 in the Racz model, 2.32 in the exponential model, and 5.38 in the Watts model.

We have shown a reciprocal relationship between irradiance and exposure time ($I_a \cdot t =$ constant) for Z100, instead of $I_a^{0.5} \cdot t =$ constant. The reciprocity between I_a and t also was found by other research groups [7,8,15,16]. Halvorson et al. found that an equal radiant exposure ($I_a \cdot t$) gave an

equivalent degree of conversion for all four of the materials they tested [15]. Similar results were found by Emami et al. [16] and Miyazaki et al. [8] on different composites. Musanje et al. [7] examined the reciprocal relationship on four different composites based on two mechanical parameters and found that one (Z250, 3M ESPE) followed the reciprocity relationship.

Some research groups have attempted to evaluate the photo-curing efficiency by using the extent of cure (curing depth) for different composite formulations [6,8,39] or for different light curing units [3,38,40,41]. Nonetheless, these studies did not report the number of photons absorbed. Stahl et al. suggested a 'integrated relative curing potential' (ICP_{rel}) parameter defined as

$$ICP_{rel} = \int_{\lambda_1}^{\lambda_2} E(\lambda)A(\lambda)d\lambda, \tag{4}$$

where $E(\lambda)$ is the relative number of photons of a curing unit, $A(\lambda)$ is the relative probability that a photon at wavelength λ will be absorbed, and $\lambda_1 - \lambda_2$ is the wavelength emission range of the curing unit [40]. In fact, if we replace $E(\lambda)$ with the actual radiant exposure inside the material and $A(\lambda)$ with the absorption coefficient $\mu_a(\lambda)$ of the material, Eq. (4) represents the total absorbed energy per unit volume in the material (with a unit of J/cm^3 according to the CIE/ISO definition [19]). Since it is difficult to measure the actual number of photons inside the materials, the Monte Carlo model provides a statistical method to find numerical and approximate solutions.

The fitted thresholds differ significantly for cured and uncured optical properties (t-test: $P < 0.05$). Based on the fitting of KHN versus radiant exposure with the Racz model, one gets $H_{KHN}^{80\%} = 3.8(0.2)$ J/cm^2 for uncured Z100, and $H_{KHN}^{80\%} = 8.8(0.6)$ J/cm^2 for cured Z100. Since in the actual situation the optical properties change as the composite polymerizes, the radiant exposure threshold required to produce 80% cure should reside between 3.8 and 8.8 J/cm^2. Observe that in Fig. 6 the area directly under the illumination received more than ten times $H_{KHN}^{80\%}$. This implies that the center cured relatively early in the irradiation and consequently would have optical properties similar to those of cured composite. Based on this argument, one can speculate that the true 80% curing threshold will be closer to the value for the cured composite because the light will propagate through the cured material for the majority of the curing process. A dynamic-optical property Monte Carlo model was not used because the relation between the number of absorbed photons and changes in optical properties is

unknown. To get the dynamic optical properties as a function of radiant exposure, one needs to use a dual channel spectrophotometer to measure the reflectance and the transmittance while at the same time applying the curing light unit. On the other hand, the step sizes in the dynamic Monte Carlo model need to be broken into many small steps due to the heterogeneous optical properties inside the materials.

In conclusions, it has been shown that one can make a reasonable approximation of the radiant exposure in photo-activated dental composite materials. In this preliminary study, only one material, Z100, was tested; therefore, more different materials need to be tested before the Monte Carlo method to predict the depth of cure and the light curing efficiency becomes available for universal use. Since the amount of light absorbed at any place within the composite is not known and is difficult to measure, the Monte Carlo simulation provides the ability to predict the light dose in any position in the composite. By knowing the exact light dose in the composite, one can further calculate the real curing efficiency and by extension may be able to predict the depth of cure. Instead of checking out the performance (hardness or DC) of every new combination of lamp and composite, Monte Carlo simulation systematically concludes the possible performance based only on the spectrum of the lamp and the optical properties of the composites. However, to make an accurate prediction using the Monte Carlo model, one needs to explicitly specify the properties of the composite (optical properties, geometry, etc.) and the light source (spectrum, geometry, etc.). Among the above conditions, the optical properties of the materials may be the most difficult to decide and be the major source of errors since the optical properties of the materials may vary during curing. Moreover, the authors have presented a simple formulation for curing that is based on reciprocity of irradiance and exposure time and the concept of a threshold radiant exposure.

Acknowledgements

References

[1] Allen EP, Bayne SC, Brodine AH, Cronin Jr RJ, Donovan TE, Kois JC, et al. Annual review of selected dental literature: report of the committee on scientific investigation of the American academy of restorative dentistry. *J Prosthet Dent* 2003;**90**:50–80.

[2] Pradhan RD, Melikechi N, Eichmiller F. The effects of irradiation wavelength bandwidth and spot size on the scraping depth and temperature rise in composite exposed to an argon laser or a conventional quartz-tungsten-halogen source. *Dent Mater* 2002;**18**:221–6.

[3] Jandt KD, Mills RW, Blackwell GB, Ashworth SH. Depth of cure and compressive strength of dental composites cured with blue light emitting diodes (LEDs). *Dent Mater* 2000;**16**:41–7.

[4] Dennison JB, Yaman P, Seir R, Hamilton JC. Effect of variable light intensity on composite shrinkage. *J Prosthet Dent* 2000;**84**:499–505.

[5] Cook WD. Factors affecting the depth of cure of UV-polymerized composites. *J Dent Res* 1980;**59**:800–8.

[6] Uhl A, Mills RW, Jandt KD. Photoinitiator dependent composite depth of cure and Knoop hardness with halogen and LED light curing units. *Biomaterials* 2003;**24**:1787–95.

[7] Musanje L, Darvell BW. Polymerization of resin composite restorative materials: exposure reciprocity. *Dent Mater* 2003;**19**:531–41.

[8] Miyazaki M, Oshida Y, Moore BK, Onose H. Effect of light exposure on fracture toughness and flexural strength of light-cured composites. *Dent Mater* 1996;**12**:328–32.

[9] Lovell LG, Newman SM, Bowman CN. The effects of light intensity, temperature, and comonomer composition on the polymerization behavior of dimethacrylate dental resins. *J Dent Res* 1999;**78**:1469–76.

[10] Oberholzer TG, Pameijer CH, Grobler SR, Rossouw RJ. The effects of different power densities and method of exposure on the marginal adaptation of four light-cured dental restorative materials. *Biomaterials* 2003;**24**:3593–8.

[11] Braga RR, Ferracane JL. Contraction stress related to degree of conversion and reaction kinetics. *J Dent Res* 2002;**81**:114–8.

[12] Sakaguchi RL, Berge HX. Reduced light energy density decrease post-gel contraction while maintaining degree of conversion in composites. *J Dent* 1998;**26**:695–700.

[13] Ferracane JL, Mitchem JC, Condon JR, Todd R. Wear and marginal breakdown of composites with various degrees of cure. *J Dent Res* 1997;**76**:1508–16.

[14] Ferracane JL. Correlation between hardness and degree of conversion during the setting reaction of unfilled dental restorative resins. *Dent Mater* 1985;**1**:11–14.

[15] Halvorson RH, Erickson RL, Davidson CL. Energy dependent polymerization of resin-based composite. *Dent Mater* 2002;**18**:463–9.

[16] Emami N, Söderholm KM. How light irradiance and curing time affect monomer conversion in light-cured resin composites. *Eur J Oral Sci* 2003;**111**:536–42.

[17] Tantbirojn D, Versluis A, Cheng Y, Douglas WH. Fracture toughness and microhardness of a composite: do they correlate? *J Dent* 2003;**31**:89–95.

[18] Cohen ME, Leonard DL, Charlton DG, Roberts HW, Ragain Jr JC. Statistical estimation of resin composite polymerization sufficiency using microhardness. *Dent Mater* 2004;**20**:158–66.

[19] Sliney DH, Wolbarsht ML. *Safety with lasers and other optical sources: a comprehensive handbook*. New York: Plenum Press; 1980.

[20] Prahl SA. Optical property measurements using the inverse adding-doubling program. OMLC, http://omlc.ogi.edu/software/iad/index.html, 1999.

[21] Prahl SA, Vangemert MJC, Welch AJ. Determining the optical properties of turbid media by using the adding-doubling method. *Appl Opt* 1993;**32**:559–68.

[22] Wilson BC, Adam G. A Monte Carlo model for the absorption and flux distributions of light in tissue. *Med Phys* 1983;**10**:824–30.

[23] Prahl SA, Keijzer M, Jacques SL, Welch AJ. A Monte Carlo model of light propagation in tissue. In: Müller GJ, Sliney D H, editors. In: *SPIE proceedings of dosimetry of laser radiation in medicine and biology*, vol. IS5, 1989. p. 102–11.

[24] Keijzer M, Jacques SL, Prahl SA, Welch AJ. Light distributions in artery tissue: Monte Carlo simulations for finite-diameter laser beams. *Lasers Surg Med* 1989;**9**:148–54.

[25] Wang L, Jacques SL, Zheng L. MCML—Monte Carlo modeling of light transport in multilayered tissues. *Comput Methods Programs Biomed* 1995;**47**:131–46.

[26] Metropolis N, Ulam S. The Monte Carlo method. *J Am Stat Assoc* 1949;**44**:335–41.

[27] Born M, Wolf E. *Principles of optics*. New York: Pergamon Press; 1980.

[28] Cook WD. Spectral distributions of dental photopolymerization sources. *J Dent Res* 1982;**61**:1436–8.

[29] Watts DC. Dental restorative materials. In: Williams DF, editor. *Materials science and technology: a comprehensive treatment, medical and dental materials*. Weinheim: VCH Verlagsgesellschaft GmbH; 1992.

[30] Racz LM, Li L, Abedian B. Cure kinetics of light-activated polymers. *J Polym Sci, Part B: Polym Phys* 1998;**36**:2887–94.

[31] Johnston WM, Leung RL, Fan PL. A mathematical model for post-irradiation hardening of photoactivated composite resins. *Dent Mater* 1985;**1**:191–4.

[32] Lloyd CH, Scrimgeour SN, Chudek JA, Hunter G, MacKay RL. The application of magnetic resonance microimaging to the visible light curing of dental resins. Part 2. Dynamic imaging by the FLASH-MOVIE pulse sequence. *Dent Mater* 2001;**17**:170–7.

[33] Lee YK, Lim BS, Kim CW. Effect of surface conditions on the color of dental resin composites. *J Biomed Mater Res* 2002;**63**:657–63.

[34] Taira M, Okazaki M, Takahashi J. Studies on optical properties of two commercial visible-light-cured composite resins by diffuse reflectance measurements. *J Oral Rehabil* 1999;**26**:329–37.

[35] Ishimaru A. *Wave propagation and scattering in random media*. New York: Academic Press, Inc.; 1978.

[36] Hapke B. *Theory of reflectance and emittance spectroscopy (Topics in Remote Sensing)*. New York: Cambridge University; 1993.

[37] Welch AJ, van Gemert M. *Optical-thermal response of laser irradiated tissue*. New York: Plenum Press; 1995.

[38] Mills RW, Uhl A, adn KD, Jandt GBB. High power light emitting diode (led) arrays versus halogen light polymerization of oral biomaterials: barcol hardness, compressive strength and radiometric properties. *Biomaterials* 2002;**23**:2955–63.

[39] Kucybala Z, Pietrzak M, Paczkowski J, Linden LA, Rabek JF. Kinetic studies of a new photoinitiator hybrid system based on camphorquinone-*n*-phenylglicyne derivatives for laser polymerization of dental restorative and stereolithographic (3d) formulations. *Polymer* 1996;**37**:4585–91.

[40] Stahl F, Ashworth SH, Mills RW. Light-emitting diode (LED) polymerization of dental composites: flexural properties and polymerization potential. *Biomaterials* 2000;**21**:1379–85.

[41] Teshima W, Nomura Y, Tanaka N, Urabe H, Okazaki M, Nahara Y. ESR study of camphorquinone/amine photoinitiator systems using blue light-emitting diodes. *Biomaterials* 2003;**24**:2097–103.